

# UCSF

## UC San Francisco Previously Published Works

### Title

Rationally Designed, Nontoxic, Nonamyloidogenic Analogues of Human Islet Amyloid Polypeptide with Improved Solubility

### Permalink

<https://escholarship.org/uc/item/9m1950xm>

### Journal

Biochemistry, 53(37)

### ISSN

0006-2960

### Authors

Wang, Hui  
Abedini, Andisheh  
Ruzsicska, Bela  
[et al.](#)

### Publication Date

2014-09-23

### DOI

10.1021/bi500592p

Peer reviewed

# Rationally Designed, Nontoxic, Nonamyloidogenic Analogues of Human Islet Amyloid Polypeptide with Improved Solubility

Hui Wang,<sup>†</sup> Andisheh Abedini,<sup>‡</sup> Bela Ruzsicska,<sup>§</sup> and Daniel P. Raleigh<sup>\*,†,||</sup>

<sup>†</sup>Department of Chemistry, State University of New York at Stony Brook, Stony Brook, New York 11794-3400, United States

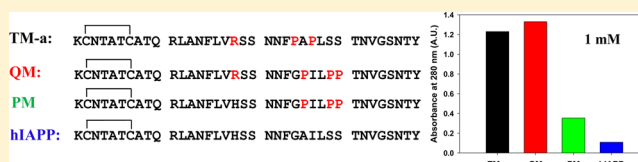
<sup>‡</sup>Diabetes Research Program, New York University School of Medicine, 522 First Avenue, New York, New York 10016, United States

<sup>§</sup>Institute for Chemical Biology and Drug Discovery, Stony Brook University, Stony Brook, New York 11794-3400, United States

<sup>||</sup>Graduate Program in Biochemistry and Structural Biology, Graduate Program in Biophysics, State University of New York at Stony Brook, Stony Brook, New York 11794-3400, United States

## Supporting Information

**ABSTRACT:** Human islet amyloid polypeptide (hIAPP or amylin) is a polypeptide hormone produced in the pancreatic  $\beta$ -cells that plays a role in glycemic control. hIAPP is deficient in type 1 and type 2 diabetes and is a promising adjunct to insulin therapy. However, hIAPP rapidly forms amyloid, and its strong tendency to aggregate limits its usefulness. The process of hIAPP amyloid formation is toxic to cultured  $\beta$ -cells and islets, and islet amyloid formation *in vivo* has been linked to  $\beta$ -cell death and islet graft failure. An analogue of hIAPP with a weakened tendency to aggregate, denoted pramlintide (PM), has been approved for clinical applications, but suffers from poor solubility, particularly at physiological pH, and its unfavorable solubility profile prevents coformulation with insulin. We describe a strategy for rationally designing analogues of hIAPP with improved properties; key proline mutations are combined with substitutions that increase the net charge of the molecule. An H18R/G24P/I26P triple mutant and an H18R/A25P/S28P/S29P quadruple mutant are significantly more soluble at neutral pH than hIAPP or PM. They are nonamyloidogenic and are not toxic to rat INS  $\beta$ -cells. The approach is not limited to these examples; additional analogues can be designed using this strategy. To illustrate this point, we show that an S20R/G24P/I26P triple mutant and an H18R/I26P double mutant are nonamyloidogenic and significantly more soluble than human IAPP or PM. These analogues and second-generation derivatives are potential candidates for the coformulation of IAPP with insulin and other polypeptides.



Insulin therapy is the most widely used treatment for diabetes. Despite improvements in insulin therapy over the past few decades, the goal of achieving complete glycemic control in diabetic patients has still not been achieved. Postprandial hyperglycemia persists in diabetes, even with aggressive insulin therapy, due, in part, to the imbalance of secreted hormones that normally work together to achieve normal glucose homeostasis.<sup>1</sup>

Human islet amyloid polypeptide (hIAPP or amylin) is a neuropancreatic hormone produced in the pancreatic  $\beta$ -cells. The polypeptide is stored in the insulin secretory granule and cosecreted with insulin.<sup>2,3</sup> Mature hIAPP is 37 residues in length and contains an amidated C-terminus and a disulfide bond between Cys-2 and Cys-7 (Figure 1). hIAPP normally complements insulin by suppressing postprandial glucagon secretion, helping to regulate the rate of gastric emptying, and inducing satiety.<sup>4–7</sup> The polypeptide forms amyloid in the pancreatic islets of Langerhans in type 2 diabetes by an unknown mechanism. hIAPP amyloid deposits are associated with reduced  $\beta$ -cell mass, and islet amyloidosis is believed to contribute to type 2 diabetes.<sup>2,8–11</sup> Islet amyloidosis also contributes to the failure of islet transplantation, and recent work has shown that prevention of islet amyloid formation enhances graft survival.<sup>12,13</sup> hIAPP also aggregates aggressively

*in vitro* and is one of the most aggregation prone naturally occurring sequences known.

hIAPP is deficient in both type 1 and type 2 diabetes patients<sup>14–16</sup> and is a promising adjunct to insulin therapy. However, clinical use of hIAPP is not practical because of its aggressive tendency to aggregate *in vitro*, leading to difficulties in formulation and storage, and because some hIAPP aggregates are toxic to  $\beta$ -cells.

Not all species form islet amyloid, and the ability to do so correlates with the primary sequence of IAPP. A number of non-amyloidogenic IAPP variants contain multiple proline substitutions, a well-known breaker of  $\beta$ -structure within the segment of residues 20–29.<sup>17,18</sup> Early work led to the suggestion that the sequence in this region controls the amyloidogenicity of the polypeptide. The situation has subsequently been shown to be more complex. Variations outside of the segment of residues 20–29 can influence significantly the amyloidogenicity of IAPP, and multiple proline substitutions in other segments of the molecule can inhibit amyloid formation.<sup>19,20</sup> In addition, the

Received: May 16, 2014

Revised: August 19, 2014

Published: August 20, 2014

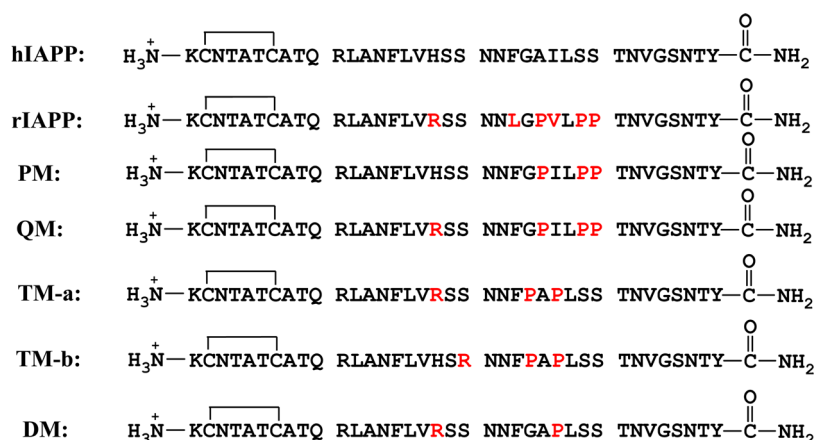


**Figure 1.** Sequences of human IAPP (hIAPP), rat IAPP (rIAPP), pramlintide (PM), H18R pramlintide (QM), H18R/G24P/I26P IAPP (TM-a), S20R/G24P/I26P IAPP (TM-b), and H18R/I26P IAPP (DM). Each peptide contains a disulfide bond connecting Cys-2 and Cys-7 and an amidated C-terminus. Residues that differ from those of human IAPP are colored red.

charge state of residue 18 and the charge state of the N-terminus play an important role in modifying the tendency to aggregate and form amyloid.<sup>21</sup> Nevertheless, substitutions within the region of residues 20–29 are very important in determining the amyloidogenicity of IAPP.<sup>20,22–24</sup> Analysis of the relationship between sequence and amyloidogenicity has led to the development of IAPP analogues, based upon rat IAPP (rIAPP), that are less prone to aggregation than hIAPP.

rIAPP differs from the human polypeptide at six positions, with five of the substitutions, including three prolines, found between residues 20 and 29. rIAPP is not toxic, does not form amyloid, and is more soluble than hIAPP, due in part to the three prolines at positions 25, 28, and 29.<sup>18,25</sup> These residues are Ala, Ser, and Ser, respectively, in the human polypeptide (Figure 1). The sequence differences between rat and human IAPP have been exploited to develop a more soluble analogue of hIAPP, pramlintide (PM, also known as Symlin), that has been clinically approved as an adjunct to insulin therapy, in which residues 25, 28, and 29 of hIAPP are substituted with proline (Figure 1). These substitutions render the human peptide nonamyloidogenic under typical conditions. Clinical studies show that PM retains the activity of hIAPP, and the addition of PM to insulin therapy improves postprandial glycemic control in patients with type 1 and type 2 diabetes.<sup>1,26–30</sup>

PM still has solubility issues, particularly at physiological pH. PM is more soluble at acidic pH where the N-terminus and His-18 will be fully protonated and is formulated under these conditions, while insulin is formulated at near neutral pH. This prevents the coformulation of insulin and PM, leading to increased cost in combination therapies and potentially reducing patient compliance, due to the need for multiple injections. There is also interest in the coformulation of IAPP or PM with other proteins, and IAPP analogues with improved solubility should be useful in this context, as well.<sup>31–33</sup>

Here, we describe an approach for rationally designing analogues of hIAPP with improved solubility that involves minimal substitutions. The strategy relies on mutating select residues to proline and making an additional substitution to increase the net charge of the molecule. We demonstrate the approach with an H18R/G24P/I26P triple mutant (TM-a) and an H18R/Ala-25/Ser-28/Ser-29 quadruple mutant (QM). Both are significantly more soluble than hIAPP or PM, and both are nonamyloidogenic and are not toxic to INS-1  $\beta$ -cells. The approach

is not limited to these two cases, and additional analogues can be designed using this strategy (Figure 1). We illustrate this point with an S20R/G24P/I26P triple mutant (TM-b) and an H18R/I26P double mutant (DM).

## MATERIALS AND METHODS

**Peptide Synthesis.** All peptides were synthesized on a 0.1 mmol scale using a CEM microwave peptide synthesizer. 9-Fluorenylmethoxycarbonyl (Fmoc) chemistry was utilized. 5-(4'-Fmoc-aminomethyl-3',5-dimethoxyphenol) valeric acid (PAL-PEG) resin was used to afford an amidated C-terminus. For hIAPP, TM-a, TM-b, and DM, Fmoc-protected pseudoproline (oxazolidine) dipeptide derivatives were incorporated to improve the yield as previously described.<sup>34</sup> For PM and QM, only Fmoc-Ala-Thr( $\Psi^{\text{Me, Me}}$ pro)-OH and Fmoc-Leu-Ser( $\Psi^{\text{Me, Me}}$ pro)-OH were utilized. Standard Fmoc reaction cycles were used as previously described.<sup>35</sup> The first residue attached to the resin, all  $\beta$ -branched residues, and all pseudoproline dipeptide derivatives were double-coupled. The peptides were cleaved from the resin using standard trifluoroacetic acid (TFA) methods.

**Oxidation and Purification of Peptides.** Crude peptides collected after cleavage were dissolved in 20% (v/v) acetic acid and lyophilized. This step was repeated several times before oxidation and purification to improve the solubility of the peptides. The peptides were oxidized in 100% dimethyl sulfoxide at room temperature to form the disulfide bond and then purified via reverse-phase high-performance liquid chromatography (RP-HPLC) using a Vydac C18 preparative column.<sup>36</sup> The masses of the pure peptides was confirmed by matrix-assisted laser desorption ionization time-of-flight mass spectrometry: hIAPP, expected 3903.6, observed 3904.6; PM, expected 3949.3, observed 3949.2; QM, expected 3969.4, observed 3968.1; TM-a, expected 3946.9, observed 3945.7; TM-b, expected 3997.4, observed, 3997.1; DM, expected 3907.3, observed, 3908.1.

**Sample Preparation.** Each peptide was dissolved in 100% hexafluoroisopropanol (HFIP) to make a 1.6 mM stock solution. Stock solutions were filtered using a 0.45  $\mu$ M Acrodisc syringe filter with a GHP membrane, and the required amount of peptide was lyophilized overnight to remove HFIP. Dry peptide was dissolved into the appropriate buffer for the fluorescence assays.

**Fluorescence Assays.** Thioflavin-T binding assays, conducted without stirring at 25 °C, were utilized to monitor amyloid formation kinetics. Fluorescence measurements were performed using a Beckman Coulter DTX 880 plate reader with a multimode detector using an excitation wavelength of 430 nm and an emission wavelength of 485 nm. Samples were prepared by dissolving the dry peptide into Tris-HCl buffer and a thioflavin-T solution immediately before the measurement. The final concentrations were 16  $\mu\text{M}$  hIAPP or 160  $\mu\text{M}$  analogue (each one) and 32  $\mu\text{M}$  thioflavin-T in 20 mM Tris-HCl (pH 7.4).

**Solubility Measurements.** Dry peptides were dissolved in PBS buffer containing 10 mM  $\text{PO}_4^{3-}$ , 137 mM NaCl, and 2.7 mM KCl (pH 7.4) at different initial concentrations and incubated for 7 days at 25 °C without being stirred. Each sample was then centrifuged using a Beckman Coulter Microfuge 22R centrifuge at 24 °C for 20 min. The relative centrifugal force used was  $1.75 \times 10^4g$ . The solubility of each sample was approximated by measuring the absorbance of the corresponding supernatant at 280 nm measured using a Beckman Coulter DU 730 UV/vis spectrophotometer. All of the peptides contain a single Tyr, three Phe residues, and a disulfide bond and no Trp; thus, their extinction coefficients at 280 nm are identical.

**Liquid Chromatography–Mass Spectroscopy (LC–MS) Experiments.** Samples were prepared by dissolving insulin, at an equimolar ratio, with either PM, DM, or TM-a in PBS buffer (pH 7.4) at an initial concentration of 500  $\mu\text{M}$ . Aliquots were removed at time zero (control). Additional aliquots were removed after incubation for 24 h and centrifuged (17500g for 20 min). Aliquots were immediately frozen with liquid nitrogen and lyophilized. LC–UV–MS measurements were taken by redissolving the samples and immediately injecting them. Samples were analyzed using an Agilent 1260 HPLC instrument and an Agilent G6224A TOF mass spectrometer. The HPLC method used a Kinetex C18 column [100 Å, 2.6  $\mu\text{m}$ , 100 mm  $\times$  2.1 mm (Phenomenex)] at 35 °C and a flow rate of 0.60 mL/min. The HPLC solvents were (A)  $\text{H}_2\text{O}$  [0.1% (v/v) acetic acid and 0.1% (v/v) TFA] and (B)  $\text{CH}_3\text{CN}$  [0.1% (v/v) acetic acid and 0.1% (v/v) TFA]. The HPLC solvent gradient consisted of the following: 10% B from 0 to 1.5 min, 10 to 50% B from 1.5 to 21.5 min, and 50 to 95% B from 21.5 to 31.5. Mass spectra were acquired in the range of  $m/z$  300–3200 with internal calibration using five standards in profile mode at 5 Hz. Electrospray ionization in the positive mode was used: cap voltage of 4000 V, gas temperature of 325 °C, drying gas of 12 L/min, nebulizer of 55 psi, and fragmentor voltage of 200 V.

UV chromatograms were acquired with a diode array detector (DAD) operating with a 10 Hz acquisition rate and a 2 nm bandwidth in the range of 205–500 nm. The absorbance was recorded at  $215 \pm 8$  and  $280 \pm 8$  nm with a 500  $\pm$  50 nm reference wavelength to obtain integrated UV areas. ESI<sup>+</sup>, TIC (total ion current) mass chromatograms were integrated, and averaged mass spectra were acquired from the integrated peaks with background subtraction. The mass spectra of the target peptides were observed in predominantly the +3 and +4 charge states. The resolution of the mass spectrometer in the described state and in this  $m/z$  range is  $\sim 13000$ . This resolution allows the isotopic distribution of the peptide  $m/z$  peaks in these charge states to be fully resolved. Mass spectra were deconvoluted using the Agilent Resolved Isotope Deconvolution algorithm. The monoisotopic, neutral masses were determined with an accuracy of  $\pm 10$  ppm. The extracted ion chromatograms (EIC)

were used with the two most intense  $m/z$  ions from the +3 and +4 charge states for relative quantitation from the mass chromatograms.

**Transmission Electron Microscopy (TEM).** TEM images were collected at the Life Science Microscopy Center at the State University of New York at Stony Brook. Aliquots (15  $\mu\text{L}$ ) of the samples used for fluorescence assays were removed at the end of each kinetic experiment, blotted on a carbon-coated 200-mesh copper grid for 1 min, and then negatively stained with saturated uranyl acetate for 1 min.

**Circular Dichroism (CD).** Far-UV CD experiments were performed on an Applied Photophysics Chirascan CD spectrophotometer at 25 °C. Aliquots from the kinetic experiments were removed at the end of each experiment, and the spectra were recorded as the average of three repeats over a range of 190–260 nm, at 1 nm intervals. A 0.1 cm quartz cuvette was used, and a background spectrum was subtracted from the data.

**Cell Culture.** Transformed rat insulinoma-1 (INS-1) pancreatic  $\beta$ -cells were grown in RPMI 1640 supplemented with 10% fetal bovine serum (FBS), 11 mM glucose, 10 mM Hepes, 2 mM L-glutamine, 1 mM sodium pyruvate, 50  $\mu\text{M}$   $\beta$ -mercaptoethanol, 100 units/mL penicillin, and 100 units/mL streptomycin. Cells were maintained at 37 °C under 5%  $\text{CO}_2$ .

**AlamarBlue Cell Viability Assays.** Cytotoxicity was measured by AlamarBlue reduction assays. INS-1  $\beta$ -cells were seeded at a density of 30000 cells/well in 96-well plates and cultured for 24 h prior to being stimulated with wild-type hIAPP and mutant IAPP peptides. Peptides dissolved in RPMI were added directly to cells and incubated on cells for 24 and 48 h. AlamarBlue was diluted 10-fold in culture media and incubated on cells for an additional 5 h at 37 °C. The fluorescence (excitation at 530 nm and emission at 590 nm) was measured on a Beckman Coulter DTX880 fluorescent plate reader. Values were calculated relative to those of control cells treated with buffer only. All values represent means  $\pm$  the standard error of the mean ( $n = 4$ ).

## RESULTS AND DISCUSSION

**Design of Soluble Analogues.** The rate of amyloid formation by hIAPP is strongly dependent on pH and is significantly faster above neutral pH, because of changes in the ionization state of the N-terminus and His-18.<sup>21,37–39</sup> PM and hIAPP both contain a His residue at position 18, while rIAPP contains an Arg. These observations led us to suspect that the solubility of PM could be significantly increased by ensuring that residue 18 remains positively charged in the pH range of interest. The two choices for substitution among the genetically encoded amino acids are Lys and Arg. Either would accomplish this goal; however, the Arg replacement is found in a number of IAPP sequences, while the Lys replacement is not. In addition, the amino group in Lys is generally more reactive than the guanidino group of Arg because of its lower  $pK_a$ ; thus, we chose to replace His-18 in the human peptide with Arg to generate the quadruple mutant, H18R/A25P/S28P/S29P IAPP, denoted QM. This mutant can also be viewed as an H18R mutant of pramlintide.

It is natural to inquire if three proline substitutions are required and if the proline substitutions need to be located at positions 25, 28, and 29; thus, we designed a second analogue that contains only two prolines in addition to the H18R substitution. A single proline mutation at position 24 or 26 of hIAPP weakens the tendency of the peptide to aggregate and converts the peptide into a moderately effective inhibitor of amyloid

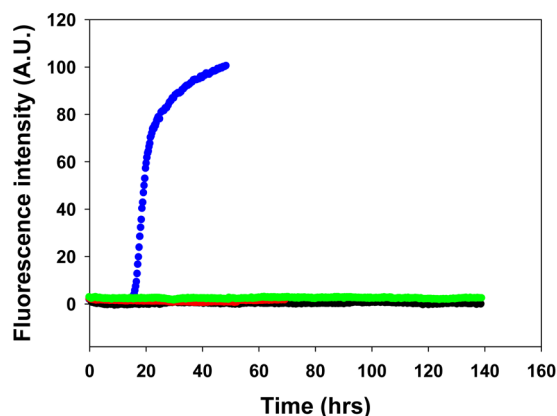


**Figure 2.** Thioflavin-T fluorescence assays of hIAPP, TM-a, QM, and PM: blue for hIAPP, black for TM-a, red for QM, and green for PM. The black, red, and green curves overlap. The experiments were conducted in 20 mM Tris-HCl (pH 7.4), without stirring at 25 °C. The concentration of hIAPP was 16  $\mu$ M. The concentration of the other peptides was 160  $\mu$ M.

formation by wild-type hIAPP.<sup>22,40</sup> The motivation for originally choosing these sites was that substitutions with proline were shown to have large effects on amyloid formation by a set of 10-residue fragments of hIAPP.<sup>41</sup> However, each of the single-proline mutants of hIAPP still forms nonamyloid aggregates at neutral pH, even at low concentrations; thus, we prepared an

analogue (TM-a) in which both residues 24 and 26 were mutated to proline and which included the H18R mutation.

**The Analogues Do Not Form Amyloid in a Homogeneous Solution.** We first tested the propensity of the different analogues to form amyloid at pH 7.4 using thioflavin-T fluorescence assays and transmission electron microscopy (TEM). Thioflavin-T is a small dye that undergoes an increase in quantum yield upon binding to amyloid fibrils and provides a convenient probe for monitoring the kinetics of amyloid formation. The dye does not perturb the kinetics of hIAPP amyloid formation under the conditions used here. Amyloid formation follows a sigmoidal time course consisting of a lag phase, in which few or no fibrils are formed, followed by a growth phase and then a saturation phase in which amyloid fibrils are in equilibrium with the soluble peptide. Amyloid formation by hIAPP reached the saturation phase within 40 h under the conditions used here, while none of the analogues tested (PM, TM-a, and QM) formed any detectable amyloid during the time course of the experiments (~140 h) as indicated by flat fluorescence curves and by TEM, even though they were examined at a concentration 10-fold higher than that of hIAPP (Figure 2). The thioflavin-T fluorescence signal derives from the fibril-bound dye, and the intensity is highly dependent on how well the dye binds; hence, thioflavin-T studies can sometimes be misleading.<sup>42</sup> Therefore, we conducted TEM measurements of the samples collected at the end of each kinetic experiment. TEM images of hIAPP showed typical

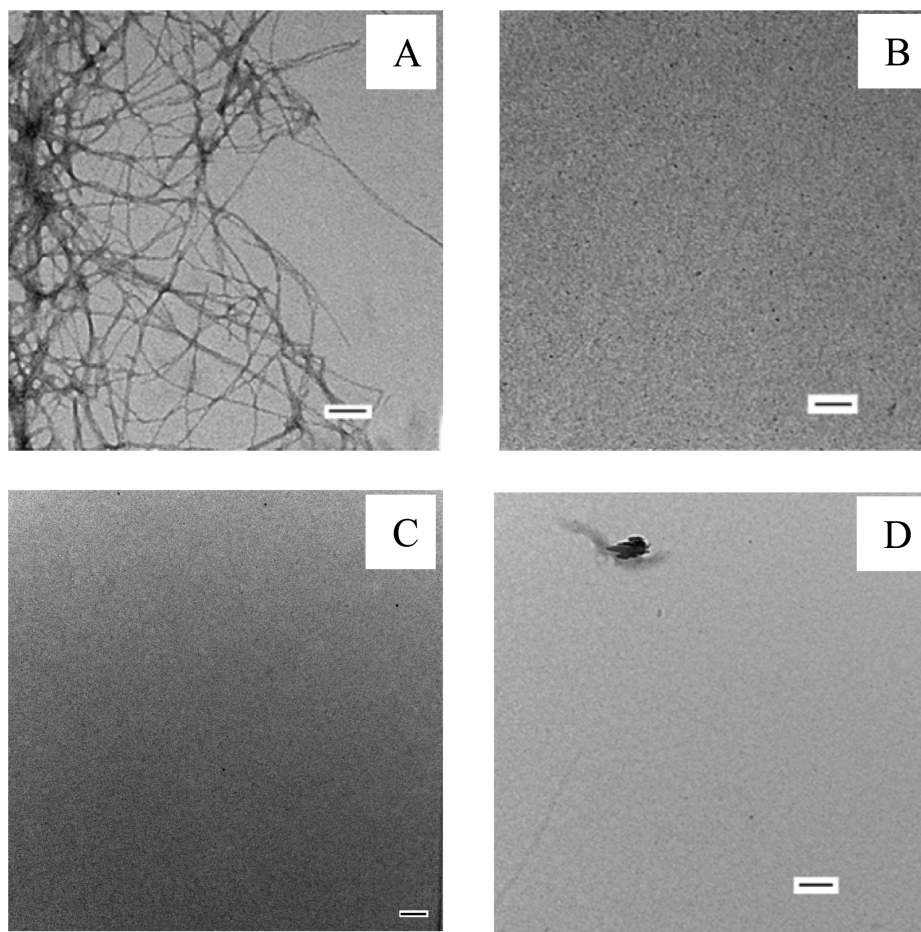


**Figure 3.** TEM images of (A) hIAPP, (B) TM-a, (C) QM, and (D) PM recorded from samples that were collected at the end of the kinetic experiments shown in Figure 2. Scale bars are 100 nm.

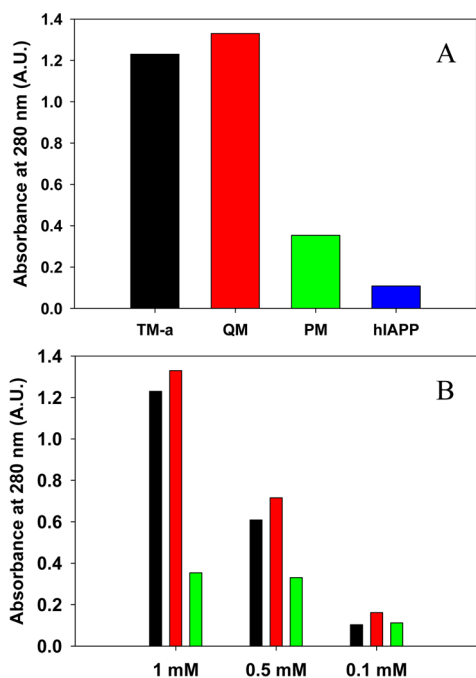


**Figure 4.** Comparison of the apparent solubilities of TM-a, QM, PM, and hIAPP. The apparent solubility in PBS buffer at pH 7.4 is represented by the absorbance at 280 nm and was measured after 7 days. (A) Amount of peptide remaining in the supernatant of samples of TM-a (black), QM (red), PM (green), and hIAPP (blue) prepared at an initial concentration of 1 mM. (B) Amount of peptide remaining in the supernatant of samples of TM-a, QM, and PM measured for different initial concentrations after incubation for 7 days. The same color coding is used as in panel A. The absorbance was measured after centrifugation at 24 °C for 20 min at  $1.75 \times 10^4g$ .

amyloid fibril morphology, while no fibrils were found in the TEM images of samples of the three analogues (PM, TM-a, and QM) (Figure 3).

**The Analogues Are Significantly More Soluble Than PM at Neutral pH.** We next compared the apparent solubilities of PM, TM-a, and QM at pH 7.4. Each peptide was incubated in PBS buffer containing 10 mM  $PO_4^{3-}$ , 137 mM NaCl, and 2.7 mM KCl for 7 days at three different initial concentrations (100  $\mu$ M, 500  $\mu$ M, and 1 mM), and the solution was then centrifuged. The apparent solubility of each sample was approximated by the absorbance of the supernatant measured at 280 nm. The extinction coefficients of all of the polypeptides are identical at 280 nm because they contain the same aromatic residues and each contains a disulfide bond; thus, the absorbance of the supernatant is a direct readout of the relative solubility of the different samples. A sample of hIAPP, prepared at an initial concentration of 1 mM, was used as a control. At 100  $\mu$ M, there were detectable differences in the amount of peptide in the soluble fraction. The supernatant of the QM sample had an absorbance, 0.16, higher than that of TM-a (0.10) or PM (0.11) (Figure 4). At higher concentrations (500  $\mu$ M and 1 mM), the amount of peptide remaining in solution was significantly higher for both analogues than for PM. At 1 mM, the absorbances of the soluble fractions of TM-a and QM were 1.2 and 1.3, respectively, while the value for the PM sample was only 0.35. In comparison, the absorbance of the supernatant of the 1 mM hIAPP sample was just 0.11 (Figure 4). For the samples prepared at an initial concentration of 500  $\mu$ M, the absorbances of the supernatants of the TM-a and QM solutions were 0.61 and 0.72, respectively, and both were significantly higher than that of PM (0.33) (Figure 4).

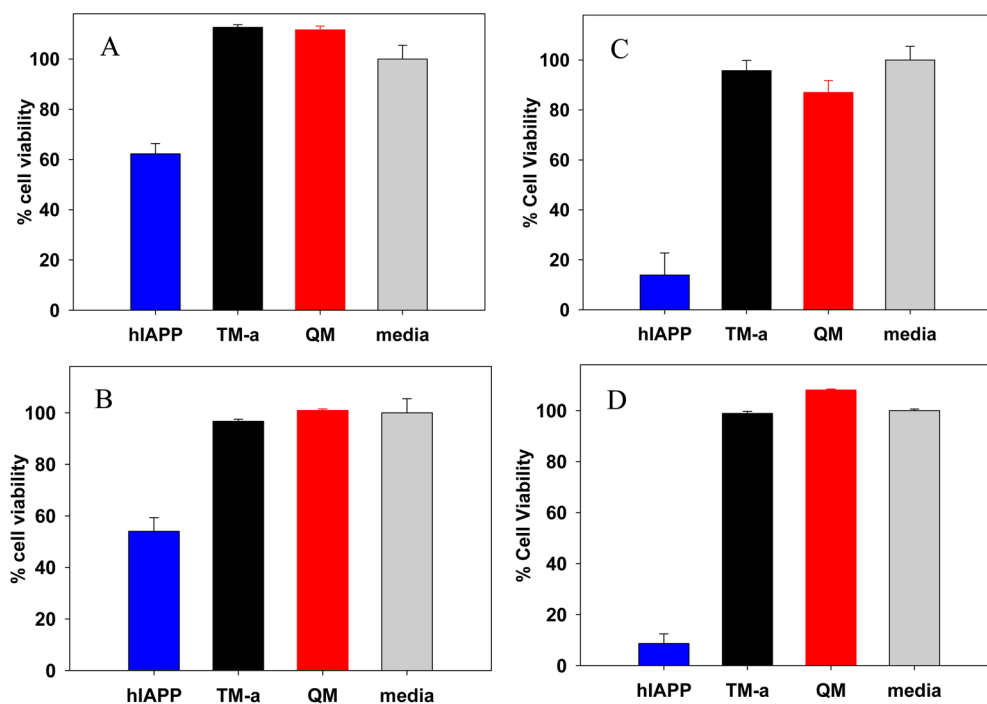


**Figure 5.** hIAPP is toxic to INS-1  $\beta$ -cells, but TM-a and QM are not. (A and B) Comparison of cell toxicity induced by hIAPP, TM-a and QM at a peptide concentration of 21  $\mu$ M. (A) Cell viability measured after incubation of cells with the peptides for 24 h. (B) Cell viability measured after incubation of cells with the peptides for 48 h. (C and D) Comparison of cell toxicity induced by the three peptides at 42  $\mu$ M. (C) Cell viability measured after incubation of cells with the peptides for 24 h. (D) Cell viability measured after incubation of cells with the peptides for 48 h. Cell viability was assessed using AlamarBlue reduction assays. Error bars represent the standard deviation determined from four repeated measurements.

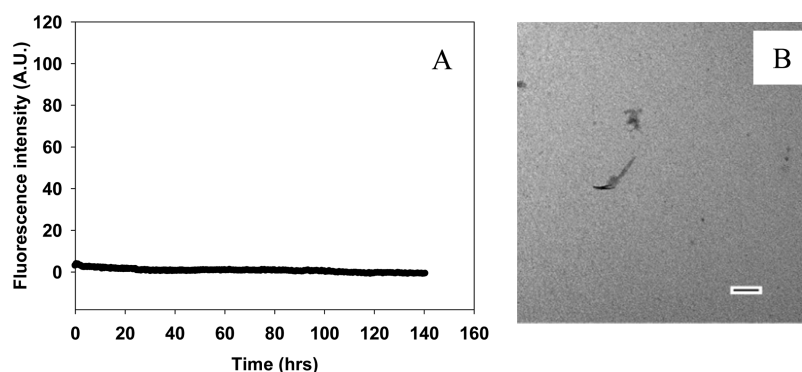


**Figure 6.** TM-b does not form amyloid, even after incubation for 140 h. (A) Thioflavin-T fluorescence assays. The kinetic experiment was conducted in 20 mM Tris-HCl (pH 7.4), without stirring at 25 °C. The concentration of TM-b was 160  $\mu$ M. (B) TEM image of a sample collected at the end of the experiment shown in panel A. The scale bar is 100 nm.

**Neither TM-a nor QM Is Toxic to  $\beta$ -Cells.** We tested the effects of the analogues on cell viability using rat INS-1  $\beta$ -cells, a pancreatic cell line that is commonly employed in studies of hIAPP toxicity. Cell viability was monitored by AlamarBlue assays for peptide samples at 21 and 42  $\mu$ M. hIAPP was used as a positive control. Incubating INS-1  $\beta$ -cells with 21  $\mu$ M hIAPP led to clearly detectable toxicity; cell viability was reduced to  $62 \pm 4\%$  relative to that of the medium alone control after incubation for 24 h and to  $54 \pm 5\%$  after incubation for 48 h. In contrast, incubation of cells with either TM-a or QM at 21  $\mu$ M barely decreased cell viability (Figure 5). Increasing the hIAPP concentration to 42  $\mu$ M resulted in even more significant effects; cell viability was reduced to only  $14 \pm 9\%$  after incubation for 24 h and  $9 \pm 9\%$  after incubation for 48 h. In striking contrast, no obvious cytotoxicity was observed for TM-a or QM at 42  $\mu$ M (Figure 5). These results demonstrate that, unlike hIAPP, TM-a and QM are not toxic to cells at the concentrations examined.

**The Strategy Can Be Extended To Include Charged Substitutions at Different Sites.** We wanted to test if a charge substitution at a different site would also lead to an enhanced solubility and reduced amyloidogenicity. We chose to target Ser-20. Substitution of a glycine at this site leads to accelerated amyloid formation, while replacement with a Lys has been shown to slow but not prevent amyloid formation.<sup>43</sup>

We prepared a S20R/G24P/I26P triple mutant (TM-b) and tested both its ability to form amyloid and its apparent solubility at neutral pH. Thioflavin-T fluorescence experiments and TEM confirmed that TM-b did not form amyloid fibrils during the time course of the experiments, even at a peptide concentration of 160  $\mu$ M (Figure 6). We then compared the apparent solubility of TM-b with PM and TM-a at pH 7.4 using the same method described above (Figure 7). TM-b was more soluble than PM and TM-a. The absorbances of the soluble fractions of samples of TM-b, TM-a, and PM prepared at an initial concentration of 100  $\mu$ M were 0.16, 0.10, and 0.11, respectively. Examination of samples prepared at higher initial concentrations revealed that TM-b was much more soluble than PM and somewhat more soluble than TM-a. We tested samples prepared at initial concentrations of 500  $\mu$ M and 1 mM. The absorbances of the supernatants of samples of TM-b prepared at initial concentrations of 500  $\mu$ M and 1 mM were 0.79 and 1.5, respectively, while the values for PM were 0.33 and 0.35, respectively.

**Multiple Proline Substitutions Are Not Required To Design Soluble Analogues.** Single-proline substitutions have

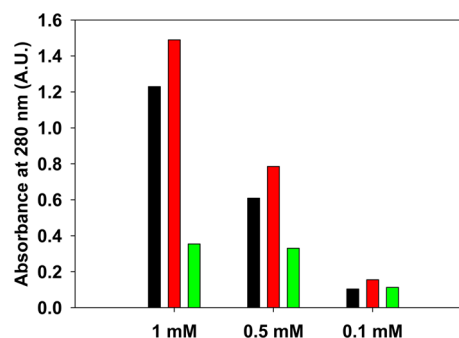


**Figure 7.** Comparison of the apparent solubility of samples of TM-a, TM-b, and PM prepared at different initial concentrations. The apparent solubility of the peptides in PBS buffer at pH 7.4 is represented by the absorbance at 280 nm and was measured after incubation for 7 days: black for TM-a, red for TM-b, and green for PM. The absorbance was measured after centrifugation at 24 °C for 20 min at  $1.75 \times 10^4$ g.

been reported to reduce the amyloidogenicity of hIAPP.<sup>22</sup> To test if multiple proline substitutions together with the charged mutations are required to improve the solubility at neutral pH, we tested an H18R/I26P double mutant of hIAPP (DM). This peptide did not form amyloid during the time course of the experiments, as demonstrated by a flat thioflavin-T fluorescence curve and by TEM (Figure 8). DM was more soluble at neutral pH than PM, even though this peptide has only one proline substitution, while PM has three (Figure 9). The absorbances of the soluble fractions of 1 mM, 500  $\mu$ M, and 100  $\mu$ M samples of DM measured after incubation for 1 week were 1.2 for the 1 mM sample, 0.67 for the 500  $\mu$ M sample, and 0.10 for the 100  $\mu$ M sample.

**Designed Analogues Are More Soluble Than Pramlintide in the Presence of Insulin.** We examined a subset of the analogues in the presence of insulin to test if they are more soluble than PM when insulin is present. We chose TM-a and DM for comparison to PM, because TM-a and DM differ from each other only at position 24, which is a proline in TM-a. Comparison of the two analogues, thus, tests if multiple Pro substitutions are required for increased solubility in the presence of insulin. The three polypeptides were individually incubated with equimolar insulin at an initial concentration of 500  $\mu$ M in PBS buffer containing 10 mM  $\text{PO}_4^{3-}$ , 137 mM NaCl, and 2.7 mM KCl at pH 7.4, and the amount of each IAPP analogue remaining in solution after 24 h was analyzed. Samples were centrifuged and aliquots of the supernatant analyzed by LC-MS.

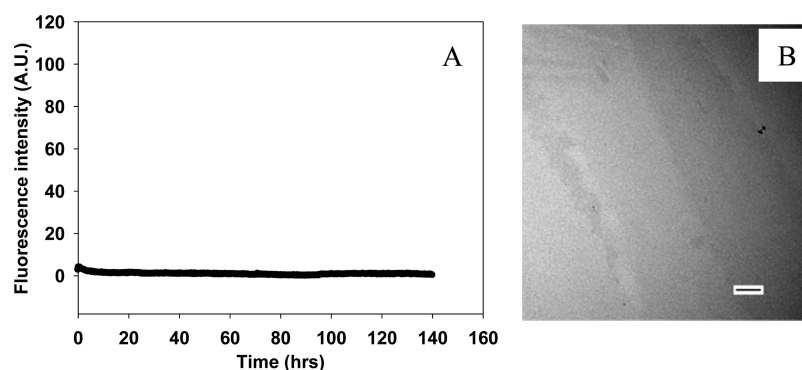


**Figure 8.** DM does not form amyloid, even after incubation for 140 h. (A) Thioflavin-T fluorescence assays. The kinetic experiment was conducted in 20 mM Tris-HCl (pH 7.4), without stirring at 25 °C. The concentration of DM was 160  $\mu$ M. (B) TEM image of a sample collected at the end of the experiments shown in panel A. The scale bar is 100 nm.

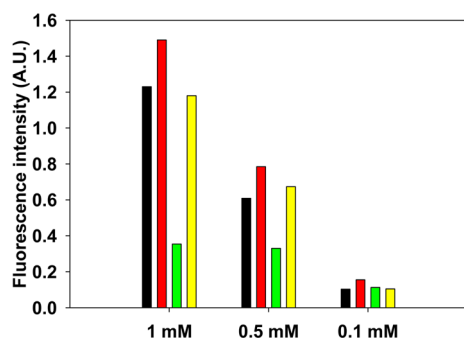


**Figure 9.** Comparison of the apparent solubilities of samples of TM-a, TM-b, PM, and DM prepared at different initial concentrations. The apparent solubility of the peptides in PBS buffer at pH 7.4 is represented by the absorbance at 280 nm and was measured after 7 days: black for TM-a, red for TM-b, green for PM, and yellow for DM. The absorbance was measured after centrifugation at 24 °C for 20 min at  $1.75 \times 10^4$ g.

Insulin could be separated from the analogues by LC (Supporting Information), allowing quantification of the amount of each IAPP analogue remaining in solution. The amount of PM in the soluble fraction was notably reduced after 24 h, with more than 37% of the material having been lost, as judged by the absorbance at 280 nm, or by the extracted ion chromatography (EIC) peak intensity (Supporting Information). The two designed analogues were more soluble than PM in the presence of insulin, and considerably less material was lost to the insoluble fraction (<15% for TM-a and <17% for DM). Any difference between the two designed analogues was modest, as judged by the absorbance of the samples, indicating that a single, strategically placed, proline together with a charge substitution is capable of generating an analogue that has improved solubility in the presence of insulin.

## CONCLUSIONS

We have developed a simple strategy for designing non-amyloidogenic, nontoxic analogues of hIAPP with solubility at neutral pH significantly better than that of PM. The strategy includes a minimum combination of mutations that increases the net charge of the peptide with single or multiple proline substitutions. Our results demonstrate that the approach is not limited to a specific site and there is no strict requirement for the number of proline substitutions. In this case, we have localized the proline substitutions within the region of residues 20–29; however, it is known that multiple proline substitutions

outside this segment can reduce amyloidogenicity, and thus, the approach may be even more general.<sup>19</sup> It is likely that N-methylated amino acids could also be used, because they, like proline, are  $\beta$ -sheet breakers.<sup>44,45</sup> Nongenetically encoded amino acids such as ornithine could likely be used instead of Lys or Arg. Of course using just the genetically encoded amino acids facilitates peptide production by recombinant means. Analogues such as the ones described here, and next-generation variants, are potential adjuncts to insulin therapy that will allow coformulation with insulin.

## ASSOCIATED CONTENT

### Supporting Information

LC chromatographs from LC–MS measurements of mixtures of insulin with PM, TM-a, and DM recorded for freshly dissolved (control, time zero) samples and for samples that were incubated for 24 h with insulin; plots showing the normalized integrated intensity of the extracted ion chromatography peak intensity of PM, TM-a, and DM for freshly dissolved (control, time zero) samples and samples that were incubated for 24 h with insulin; and plots showing the normalized integrated absorbance at 280 nm of PM, TM-a, and DM for freshly dissolved (control, time zero) samples and samples that were incubated for 24 h with insulin. This material is available free of charge via the Internet at <http://pubs.acs.org>.

## AUTHOR INFORMATION

### Corresponding Author

\*E-mail: [daniel.raleigh@stonybrook.edu](mailto:daniel.raleigh@stonybrook.edu). Phone: (631) 632-9547. Fax: (631) 632-7960.

### Funding

This work was supported by National Institutes of Health Grant GM078114 to D.P.R.

### Notes

The authors declare a competing financial interest. A patent for the design and application of soluble IAPP analogues has been submitted.

## ACKNOWLEDGMENTS

We thank Dr. Ping Cao for assistance with the toxicity assays. We thank Mr. Tyler Wilkinson for assistance with peptide synthesis and purification.



## ■ ABBREVIATIONS

CD, circular dichroism; DM, H18R/I26P double mutant; EIC, extracted ion chromatograms; FBS, fetal bovine serum; Fmoc, 9-fluorenylmethoxycarbonyl; HFIP, hexafluoroisopropanol; hIAPP, human islet amyloid polypeptide; INS-1, rat insulinoma-1; LC-MS, liquid chromatography-mass spectrometry; PAL-PEG, 5-(4'-Fmoc-aminomethyl-3',5-dimethoxyphenyl) valeric acid; PM, pramlintide; QM, H18R/Ala-25/Ser-28/Ser-29 quadruple mutant; rIAPP, rat IAPP; RP-HPLC, reverse-phase high-performance liquid chromatography; TEM, transmission electron microscopy; TM-a, H18R/G24P/I26P triple mutant; TM-b, S20R/G24P/I26P triple mutant.

## ■ REFERENCES

- (1) Kruger, D. F., and Gloster, M. A. (2004) Pramlintide for the treatment of insulin-requiring diabetes mellitus: Rationale and review of clinical data. *Drugs* 64, 1419–1432.
- (2) Cooper, G. J., Willis, A. C., Clark, A., Turner, R. C., Sim, R. B., and Reid, K. B. (1987) Purification and characterization of a peptide from amyloid-rich pancreases of type 2 diabetic patients. *Proc. Natl. Acad. Sci. U.S.A.* 84, 8628–8632.
- (3) Clark, A., Lewis, C. E., Willis, A. C., Cooper, G. J. S., Morris, J. F., Reid, K. B. M., and Turner, R. C. (1987) Islet amyloid formed from diabetes-associated peptide may be pathogenic in type-2 diabetes. *Lancet* 2, 231–234.
- (4) Gedulin, B. R., Rink, T. J., and Young, A. A. (1997) Dose-response for glucagonostatic effect of amylin in rats. *Metabolism* 46, 67–70.
- (5) Rushing, P. A., Hagan, M. M., Seeley, R. J., Lutz, T. A., D'Alessio, D. A., Air, E. L., and Woods, S. C. (2001) Inhibition of central amylin signaling increases food intake and body adiposity in rats. *Endocrinology* 142, 5035–5038.
- (6) Clementi, G., Caruso, A., Cutuli, V. M. C., deBernardis, E., Prato, A., and AmicoRoxas, M. (1996) Amylin given by central or peripheral routes decreases gastric emptying and intestinal transit in the rat. *Experientia* 52, 677–679.
- (7) Scherbaum, W. A. (1998) The role of amylin in the physiology of glycemic control. *Exp. Clin. Endocrinol. Diabetes* 106, 97–102.
- (8) Westermark, P., Wernstedt, C., O'Brien, T. D., Hayden, D. W., and Johnson, K. H. (1987) Islet amyloid in type 2 human diabetes mellitus and adult diabetic cats contains a novel putative polypeptide hormone. *Am. J. Pathol.* 127, 414–417.
- (9) Clark, A., Wells, C. A., Buley, I. D., Cruickshank, J. K., Vanhegan, R. L., Matthews, D. R., Cooper, G. J., Holman, R. R., and Turner, R. C. (1988) Islet amyloid, increased A-cells, reduced B-cells and exocrine fibrosis: Quantitative changes in the pancreas in type 2 diabetes. *Diabetes Res. Clin. Pract.* 9, 151–159.
- (10) Westermark, P., and Grimelius, L. (1973) Pancreatic-islet cells in insular amyloidosis in human diabetic and non-diabetic adults. *AActa Pathol. Microbiol. Immunol. Scand., Sect. A* 81, 291–300.
- (11) Westermark, P., and Wilander, E. (1978) The influence of amyloid deposits on the islet volume in maturity onset diabetes mellitus. *Diabetologia* 15, 417–421.
- (12) Andersson, A., Bohman, S., Borg, L. A., Paulsson, J. F., Schultz, S. W., Westermark, G. T., and Westermark, P. (2008) Amyloid deposition in transplanted human pancreatic islets: A conceivable cause of their long-term failure. *Exp. Diabetes Res.* 2008, 562985.
- (13) Potter, K. J., Abedini, A., Marek, P., Klimek, A. M., Butterworth, S., Driscoll, M., Baker, R., Nilsson, M. R., Warnock, G. L., Oberholzer, J., Bertera, S., Trucco, M., Korbitt, G. S., Fraser, P. E., Raleigh, D. P., and Verchere, C. B. (2010) Islet amyloid deposition limits the viability of human islet grafts but not porcine islet grafts. *Proc. Natl. Acad. Sci. U.S.A.* 107, 4305–4310.
- (14) Koda, J. E., Fineman, M., Rink, T. J., Dailey, G. E., Muchmore, D. B., and Linarelli, L. G. (1992) Amylin concentrations and glucose control. *Lancet* 339, 1179–1180.
- (15) Fineman, M. S., Giotta, M. P., Thompson, R. G., Kolterman, O. K., and Koda, J. E. (1996) Amylin response following Sustacal(R) ingestion is diminished in type II diabetic patients treated with insulin. *Diabetologia* 39, 566.
- (16) Kruger, D. F., Gatcomb, P. M., and Owen, S. K. (1999) Clinical implications of amylin and amylin deficiency. *Diabetes Educ.* 25, 389–397.
- (17) Westermark, P., Engstrom, U., Johnson, K. H., Westermark, G. T., and Betsholtz, C. (1990) Islet amyloid polypeptide: Pinpointing amino acid residues linked to amyloid fibril formation. *Proc. Natl. Acad. Sci. U.S.A.* 87, 5036–5040.
- (18) Westermark, P., Andersson, A., and Westermark, G. T. (2011) Islet amyloid polypeptide, islet amyloid, and diabetes mellitus. *Physiol. Rev.* 91, 795–826.
- (19) Abedini, A., and Raleigh, D. P. (2006) Destabilization of human IAPP amyloid fibrils by proline mutations outside of the putative amyloidogenic domain: Is there a critical amyloidogenic domain in human IAPP? *J. Mol. Biol.* 355, 274–281.
- (20) Fox, A., Snollaerts, T., Errecart Casanova, C., Calciano, A., Nogaj, L. A., and Moffet, D. A. (2010) Selection for nonamyloidogenic mutants of islet amyloid polypeptide (IAPP) identifies an extended region for amyloidogenicity. *Biochemistry* 49, 7783–7789.
- (21) Abedini, A., and Raleigh, D. P. (2005) The role of His-18 in amyloid formation by human islet amyloid polypeptide. *Biochemistry* 44, 16284–16291.
- (22) Abedini, A., Meng, F. L., and Raleigh, D. P. (2007) A single-point mutation converts the highly amyloidogenic human islet amyloid polypeptide into a potent fibrillization inhibitor. *J. Am. Chem. Soc.* 129, 11300–11301.
- (23) Chakraborty, S., Mukherjee, B., and Basu, S. (2013) Pinpointing proline substitution to be responsible for the loss of amyloidogenesis in IAPP. *Chem. Drug Des.* 82, 446–452.
- (24) Buchanan, L. E., Dunkelberger, E. B., Tran, H. Q., Cheng, P. N., Chiu, C. C., Cao, P., Raleigh, D. P., de Pablo, J. J., Nowick, J. S., and Zanni, M. T. (2013) Mechanism of IAPP amyloid fibril formation involves an intermediate with a transient  $\beta$ -sheet. *Proc. Natl. Acad. Sci. U.S.A.* 110, 19285–19290.
- (25) Cao, P., Meng, F., Abedini, A., and Raleigh, D. P. (2010) The ability of rodent islet amyloid polypeptide to inhibit amyloid formation by human islet amyloid polypeptide has important implications for the mechanism of amyloid formation and the design of inhibitors. *Biochemistry* 49, 872–881.
- (26) Weyer, C., Maggs, D. G., Young, A. A., and Kolterman, O. G. (2001) Amylin replacement with pramlintide as an adjunct to insulin therapy in type 1 and type 2 diabetes mellitus: A physiological approach toward improved metabolic control. *Curr. Pharm. Des.* 7, 1353–1373.
- (27) Fineman, M., Weyer, C., Maggs, D. G., Strobel, S., and Kolterman, O. G. (2002) The human amylin analog, pramlintide, reduces postprandial hyperglucagonemia in patients with type 2 diabetes mellitus. *Horm. Metab. Res.* 34, 504–508.
- (28) Fineman, M. S., Koda, J. E., Shen, L. Z., Strobel, S. A., Maggs, D. G., Weyer, C., and Kolterman, O. G. (2002) The human amylin analog, pramlintide, corrects postprandial hyperglucagonemia in patients with type I diabetes. *Metabolism* 51, 636–641.
- (29) Kleppinger, E. L., and Vivian, E. M. (2003) Pramlintide for the treatment of diabetes mellitus. *Ann. Pharmacother.* 37, 1082–1089.
- (30) Schmitz, O., and Brock, B. (2004) Amylin agonists: A novel approach in the treatment of diabetes. *Diabetes* 53, S233–S238.
- (31) Seth, R., Terry, D. E., Parrish, B., Bhatt, R., and Overton, J. M. (2012) Amylin-leptin coadministration stimulates central histaminergic signaling in rats. *Brain Res.* 1442, 15–24.
- (32) Trevaskis, J. L., Lei, C., Koda, J. E., Weyer, C., Parkes, D. G., and Roth, J. D. (2010) Interaction of leptin and amylin in the long-term maintenance of weight loss in diet-induced obese rats. *Obesity* 18, 21–26.
- (33) Roth, J. D., Roland, B. L., Cole, R. L., Trevaskis, J. L., Weyer, C., Koda, J. E., Anderson, C. M., Parkes, D. G., and Baron, A. D. (2008) Leptin responsiveness restored by amylin agonism in diet-induced

obesity: Evidence from nonclinical and clinical studies. *Proc. Natl. Acad. Sci. U.S.A.* 105, 7257–7262.

(34) Abedini, A., and Raleigh, D. P. (2005) Incorporation of pseudoproline derivatives allows the facile synthesis of human IAPP, a highly amyloidogenic and aggregation-prone polypeptide. *Org. Lett.* 7, 693–696.

(35) Marek, P., Woys, A. M., Sutton, K., Zanni, M. T., and Raleigh, D. P. (2010) Efficient microwave-assisted synthesis of human islet amyloid polypeptide designed to facilitate the specific incorporation of labeled amino acids. *Org. Lett.* 12, 4848–4851.

(36) Abedini, A., Singh, G., and Raleigh, D. P. (2006) Recovery and purification of highly aggregation-prone disulfide-containing peptides: Application to islet amyloid polypeptide. *Anal. Biochem.* 351, 181–186.

(37) Tu, L.-H., Serrano, A. L., Zanni, M. T., and Raleigh, D. P. (2014) Mutational analysis of preamyloid intermediates: The role of His-Tyr interactions in islet amyloid formation. *Biophys. J.* 106, 1520–1527.

(38) Jha, S., Snell, J. M., Sheftic, S. R., Patil, S. M., Daniels, S. B., Kolling, F. W., and Alexandrescu, A. T. (2014) pH dependence of amylin fibrillization. *Biochemistry* 53, 300–310.

(39) Charge, S. B. P., Dekoning, E. J. P., and Clark, A. (1995) Effect of pH and insulin on fibrillogenesis of islet amyloid polypeptide in vitro. *Biochemistry* 34, 14588–14593.

(40) Meng, F. L., Raleigh, D. P., and Abedini, A. (2010) Combination of kinetically selected inhibitors in trans leads to highly effective inhibition of amyloid formation. *J. Am. Chem. Soc.* 132, 14340–14342.

(41) Moriarty, D. F., and Raleigh, D. P. (1999) Effects of sequential proline substitutions on amyloid formation by human amylin<sub>20–29</sub>. *Biochemistry* 38, 1811–1818.

(42) Meng, F. L., Marek, P., Potter, K. J., Verchere, C. B., and Raleigh, D. P. (2008) Rifampicin does not prevent amyloid fibril formation by human islet amyloid polypeptide but does inhibit fibril thioflavin-T interactions: Implications for mechanistic studies of  $\beta$ -cell death. *Biochemistry* 47, 6016–6024.

(43) Cao, P., Tu, L. H., Abedini, A., Levsh, O., Akter, R., Patsalo, V., Schmidt, A. M., and Raleigh, D. P. (2012) Sensitivity of amyloid formation by human islet amyloid polypeptide to mutations at residue 20. *J. Mol. Biol.* 421, 282–295.

(44) Yan, L.-M., Velkova, A., Tatarek-Nossol, M., Rammes, G., Sibaev, A., Andreetto, E., Kracklauer, M., Bakou, M., Malideli, E., Göke, B., Schirra, J., Storr, M., and Kapurniotu, A. (2013) Selectively N-methylated soluble IAPP mimics as potent IAPP receptor agonists and nanomolar inhibitors of cytotoxic self-assembly of both IAPP and A $\beta$ 40. *Angew. Chem., Int. Ed.* 52, 10378–10383.

(45) Yan, L.-M., Tatarek-Nossol, M., Velkova, A., Kazantzis, A., and Kapurniotu, A. (2006) Design of a mimic of nonamyloidogenic and bioactive human islet amyloid polypeptide (IAPP) as nanomolar affinity inhibitor of IAPP cytotoxic fibrillogenesis. *Proc. Natl. Acad. Sci. U.S.A.* 103, 2046–2051.